

Enhanced Generative Data Augmentation for Semantic Segmentation via Stronger Guidance

Quang-Huy Che^{1,2}, Duc-Tri Le^{1,2} and Vinh-Tiep Nguyen^{1,2}

¹University of Information Technology, Ho Chi Minh City, Vietnam

²Vietnam National University, Ho Chi Minh City, Vietnam

huycq@uit.edu.vn, 21522526@gm.uit.edu.vn, tiepvn@uit.edu.vn

Keywords: Data Augmentation, Stable Diffusion, Semantic Segmentation

Abstract: Data augmentation is a widely used technique for creating training data for tasks that require labeled data, such as semantic segmentation. This method benefits pixel-wise annotation tasks requiring much effort and intensive labor. Traditional data augmentation methods involve simple transformations like rotations and flips to create new images from existing ones. However, these new images may lack diversity along the main semantic axes in the data and not change high-level semantic properties. To address this issue, generative models have emerged as an effective solution for augmenting data by generating synthetic images. Controllable generative models offer a way to augment data for semantic segmentation tasks using a prompt and visual reference from the original image. However, using these models directly presents challenges, such as creating an effective prompt and visual reference to generate a synthetic image that accurately reflects the content and structure of the original. In this work, we introduce an effective data augmentation method for semantic segmentation using the Controllable Diffusion Model. Our proposed method includes efficient prompt generation using *Class-Prompt Appending* and *Visual Prior Combination* to enhance attention to labeled classes in real images. These techniques allow us to generate images that accurately depict segmented classes in the real image. In addition, we employ the *class balancing algorithm* to ensure efficiency when merging the synthetic and original images to generate balanced data for the training dataset. We evaluated our method on the PASCAL VOC datasets and found it highly effective for synthesizing images in semantic segmentation.

1 INTRODUCTION

Semantic segmentation is a fundamental computer vision task that involves classifying each pixel in an image. Deep learning models have significantly advanced semantic segmentation methods. These models are usually trained on large-scale datasets with dense annotations, such as PASCAL VOC (Everingham et al., 2015), MS COCO (Lin et al., 2014), BDD100K (Yu et al., 2020), and ADE20K (Zhou et al., 2019). It is often necessary to re-label the data to address a specific task. However, labeling a new dataset to enable accurate model learning is time-consuming and costly, particularly for semantic segmentation tasks that require pixel-level labeling.

An alternative to enhancing data diversity without annotating a new dataset is data augmentation, which creates more training examples by leveraging an existing dataset. Commonly used data augmentation methods in semantic segmentation include rotating, scaling, flipping, and other manipulations of individ-

ual images. These techniques encourage the model to learn more invariant features, thereby improving the robustness of the trained model. However, basic transformations do not produce novel structural elements, textures, or changes in perspective. Consequently, more advanced data augmentation methods utilize generative models for different tasks, such as those described in the following works (Trabucco et al., 2024; Azizi et al., 2023; He et al., 2023; Fang et al., 2024; Wu et al., 2024). Generative models leverage the ability to create new images based on inputs such as text, semantic maps, and image guidance (edge, line art, soft edge) to specific tasks and data augmentation needs. Notably, Stable Diffusion (SD) (Rombach et al., 2022; Podell et al., 2024) and its variants (Zhang et al., 2023; Mou et al., 2023) excel in producing high-quality images based on input conditions.

The segmentation mask annotation can be easily computed in data augmentation using simple transformations. However, with generative models, data

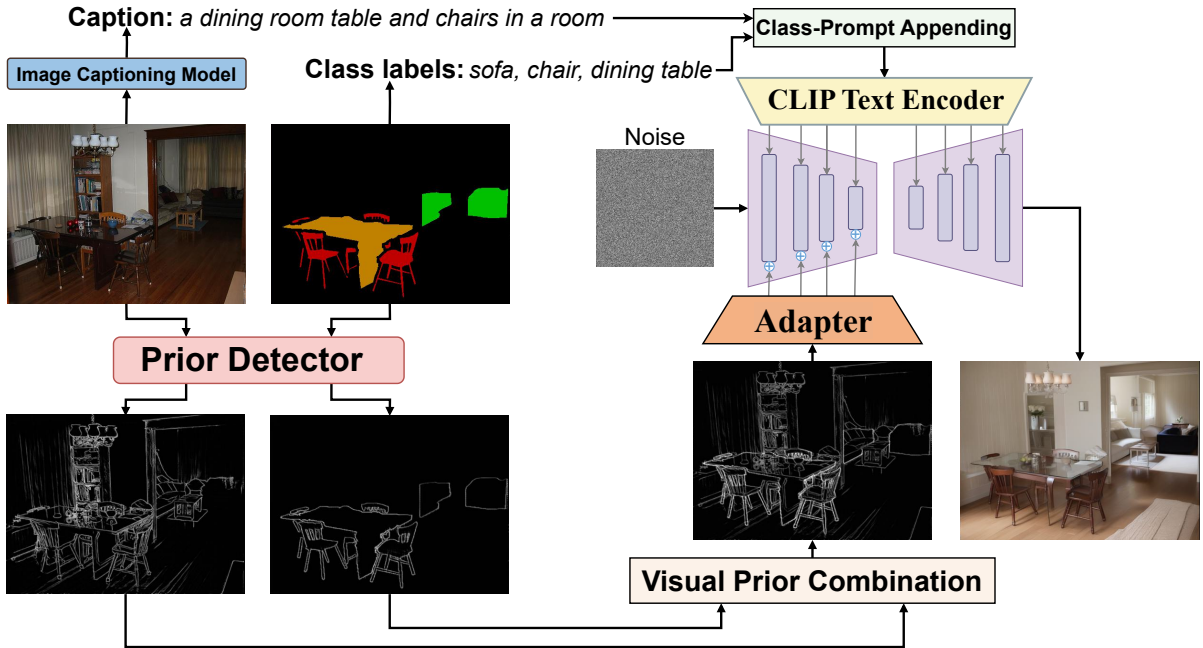


Figure 1: The controllable data augmentation pipeline for the semantic segmentation task combines our proposed methods: Class-Prompt Appending and Visual Prior Combination

augmentation is more problematic as it requires generating new images while still matching the segmentation mask. A simple approach to the aforementioned challenge is to use Inpainting model (Rombach et al., 2022) to change the labeled classes in the images while preserving the remaining information. Although it can increase the diversity of the data classes, the diversity of the surrounding elements is limited when applying the method above. In addition, some studies (Mou et al., 2023; Zhang et al., 2023; Chae et al., 2023) propose image generation models that can be controlled from the segmentation mask of the image. However, all the above-mentioned methods require training on semantic segmentation datasets for generative models, which results in the model being unable to generate classes that are not part of the trained dataset.

With a deep understanding of pre-trained generative models, we can identify their strengths with a vast knowledge base, such as generality and good controllability. In this paper, we propose using controllable generative models with prior visual without training on semantic segmentation datasets to augment data for semantic segmentation. The proposed methods ensure that the generated images match the original images in terms of the number of labels and their localizations but with transformations in color, context, and style. To achieve high performance in data augmentation, we propose Visual Prior Combination

and Class-Prompt Appending to enhance the visual representation of labeled classes. This combination method is depicted in Figure 1. In addition, we also use class balancing algorithm to control the number of classes during image generation so that when combining the synthetic dataset and the original data, the classes in the extended dataset are more balanced.

2 RELATED WORK

Data augmentation using generative models is commonly applied in classification tasks (Trabucco et al., 2024; Azizi et al., 2023; He et al., 2023). Unlike classification tasks, to augment data for Segmentation or Object Detection tasks, where the synthetic images must ensure the location of the objects, Inpainting model (Rombach et al., 2022) is considered an option because it allows to specify what to edit as a mask. However, because it is only possible to edit objects in the mask, the contexts around the object are almost kept the same, which leads to the synthetic images needing to be more diverse in terms of content.

Some studies (Mou et al., 2023; Zhang et al., 2023; Chae et al., 2023) suggest using semantic segmentation maps to guide image generation. This means labeling each pixel to show which class it belongs to, helping to create accurate images with correct object locations and details. However, these

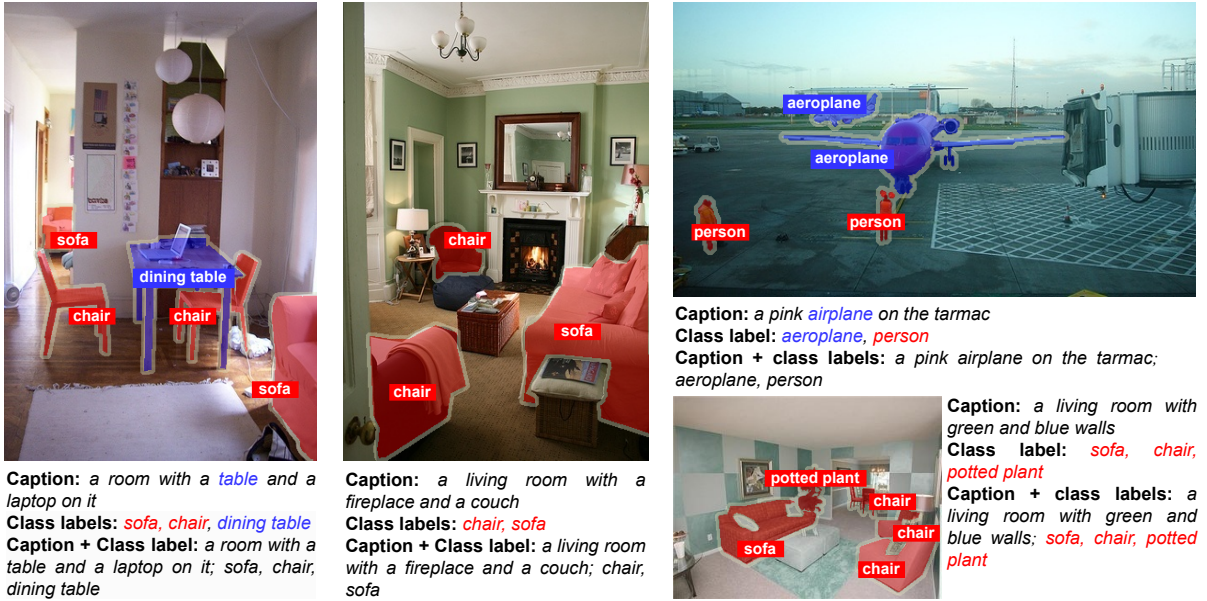


Figure 2: Common issues of the generated prompt. Red describes the missing classes in the generated prompt while blue marks the ones appearing in the sentence.

methods need to be trained on segmentation datasets. This limits the synthetic images to only the trained classes and makes them unclear for untrained classes. For example, the method in (Mou et al., 2023; Zhang et al., 2023) is trained on the ADE20K (Zhou et al., 2019) dataset, which has various images from different contexts like indoor, outdoor, industrial, and natural scenes. Suppose we need to generate synthetic images for the BDD100K dataset (Yu et al., 2020), which includes images from vehicle cameras. In that case, the model can not generate new classes not in the ADE20K dataset, such as traffic signs, traffic lights, and road markings. Because of this limitation, we do not use models guided by semantic segmentation maps in this study to keep our method general.

Instead of directly selecting synthetic images to train the model, some studies (Fang et al., 2024; Wu et al., 2024) propose using post-filtering techniques to choose the best synthetic images. However, selecting one high-quality image from many can be time-consuming, and imperfect filtering can lead to a low-quality synthetic dataset. In addition, with the ability to generate different images from the same input and change the random seeds, selecting the best ones based on multiple results does not accurately reflect the image generation ability. Therefore, in this paper, we directly use the generated images without going through any post-filtering techniques to demonstrate the effectiveness of the proposed method. In addition, in Section 4.3, we also integrate the filter using CLIP Encoder (Fang et al., 2024) to demonstrate the

compatibility of the proposed method when applying filters.

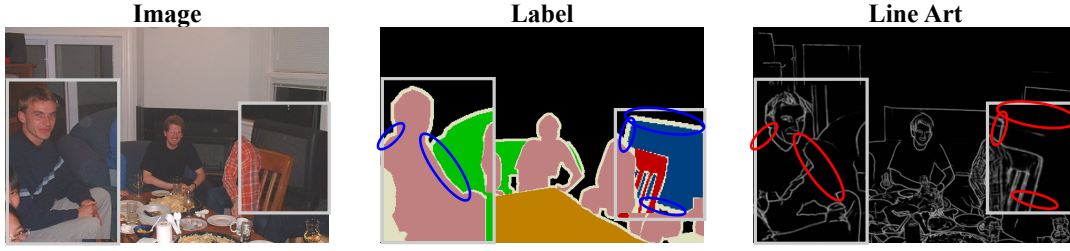
3 METHOD

Our proposed image data augmentation pipeline is shown in Figure 1, which consists of three main components: (1) Text prompt construction, (2) Visual Prior Combination, and (3) Controllable Diffusion Generation. *Class-Prompt Appending* append “class prompt” including the classes visible in the image with “caption” generated from the Image Caption model. *Visual Pre-Matching* combines the visual pre-information of the real image and the segmentation map. The results of the above two methods are fed into the Controllable Steady Diffusion model to generate the synthetic image. In addition, to generate synthetic data from a given dataset, we using *class balancing algorithm* to generate data with even distribution among classes. Next, we provide a detailed description of each component.

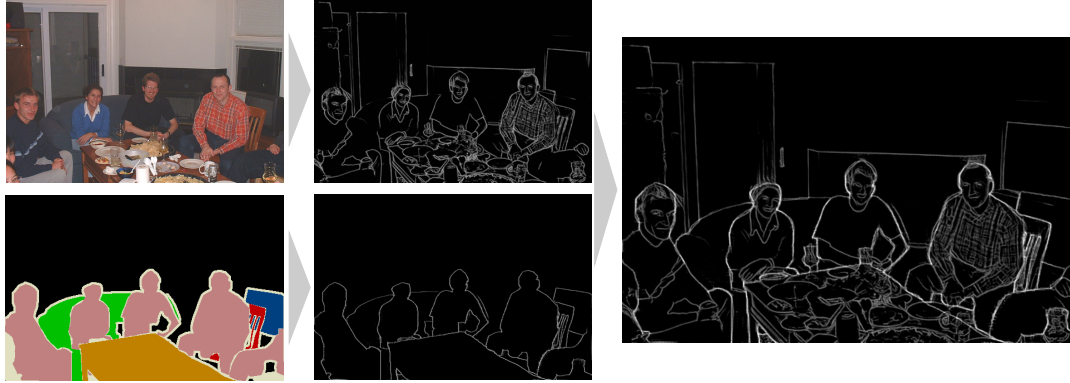
3.1 Preliminary

The diffusion models comprise both forward and reverse processes (Ho et al., 2020). In the forward process, a Markovian chain is defined with noise added to the clean image x_0 :

$$x_t = \sqrt{\bar{\alpha}_t}x_0 + \sqrt{1 - \bar{\alpha}_t}\varepsilon, \quad \varepsilon \sim \mathcal{N}(0, I) \quad (1)$$



(a) An example of information loss occurs when using Line Art Detection, particularly in the reddish areas, where information is lacking.



(b) The results of the Visual Prior Combination method demonstrate that previously edge-deficient objects are now fully detailed, and the edge features of the labeled classes are more prominent compared to the background, thereby enhancing the generative model’s attention capability.

Figure 3: The edge feature results before (a) and after (b) using the Visual Prior Combination method..

where x_t is the noise image at time step t , ε is a noise map sampled from a Gaussian distribution, and $\bar{\alpha}_t$ denotes the corresponding noise level. The neural network ε_t is parameterized by θ , which is optimized to predict the noise added to ε_t in the reverse process. A classical diffusion model is typically optimized by:

$$\mathcal{L}_{DDPM} = \mathbb{E}_{x_0, t, \varepsilon_t} \|\varepsilon_t - \varepsilon_\theta(x_t, t)\|_2^2 \quad (2)$$

In the context of controllable generation (Zhang et al., 2023; Mou et al., 2023), when given a condition image c_v and a text prompt c_t , the diffusion training loss function at time t can be re-written as:

$$\mathcal{L} = \mathbb{E}_{x_0, c_v, c_t, t, \varepsilon_t} \|\varepsilon_t - \varepsilon_\theta(x_t, t, c_v, c_t)\|_2^2 \quad (3)$$

3.2 Generative Data Augmentation Pipeline

3.2.1 Text prompt construction

To generate an image containing the labeled classes as in the original image, we need a robust prompt that describes the original image well to serve as input to the SD model. One way to do this is by construct-

ing a prompt based on the labeled classes. For example, if image I_i contains target classes $C_i = [c_1, \dots, c_M]$, where M is the number of classes in image I_i , we can construct a simple prompt such as: “ c_1, \dots, c_M ” or “An image of c_1, \dots, c_M ”. However, using a prompt that solely lists target classes doesn’t clearly describe the original image’s layout. In this case, we can employ the existing or generated captions from the training images in these datasets as text prompts for Stable Diffusion. For example, we can use the provided captions when using the COCO dataset (Lin et al., 2014). However, most datasets, such as PASCAL VOC (Everingham et al., 2015), BDD100K (Yu et al., 2020), and ADE20K (Zhou et al., 2019), do not have captions, while annotating captions for images also requires intensive labor. Therefore, we propose using an image captioning model such as BLIP-2 (Li et al., 2023) to generate captions for each image. However, we encountered some issues with the generated annotations; many did not include all the actual classes in the images (as illustrated in Figure 2). This issue leads to missing class names in the captions.

To address the abovementioned limitations, we propose combining the generated captions with the class labels of the images, as suggested in (Nguyen

et al., 2023). With an image I_i , we append the generated captions \mathcal{P}_i^g with the class labels \mathcal{P}_i^c to generate new text prompts \mathcal{P}_i^* . This process, known as *class-prompt appending*, can be represented as: $\mathcal{P}_i^* = \langle \mathcal{P}_i^g; \mathcal{P}_i^c \rangle$. For example, in the sub-figure in the top-right corner of Figure 2, the prompt generated by our proposed method would be “a pink plane on the tarmac; aeroplane, person”. Our method ensures that new text prompts include both general information and the target classes of the original image. This technique helps the synthetic image to have a clear layout similar to the original one and also addresses the problem of missing labeled classes in the synthetic image.

3.2.2 Visual Prior Combination

Unlike Stable Diffusion models that typically only use text prompts to generate images, Controllable Generation models require additional input guidance (Canny Edge (Canny, 1986), Sketch-Guided (Su et al., 2021), Line-Art Edge (Chan et al., 2022), Depth Map (Ranftl et al., 2022), HED soft edge (Xie and Tu, 2015)) generated from the visual prior to determine the image layout. Canny, line-art edge and sketch are the visual priors we propose using to balance the diversity of the image and the precise localization of the generated classes in the image. Our default visual prior is Line-Art Edge to generate visual guidance. In Section 4.3.5, we also discuss other types of visual priors to see how effectively they augment the data. Using the T2I-Adapter (Mou et al., 2023) model, the Linear Detector converts the image into visual prior in-line drawings for each input image. Then, the Adapter generates different resolution features, performing conditional operations at each time step with the UNet denoiser’s features.

In general, methods such as Line-Art Edge, Canny Edge, HED soft edge all suffer from the limitation that the labeled classes in the image may be blurred or small in size, leading to inaccuracies in describing the shape of the labeled classes within the conditional image. Figure 3a shows an image produced using Line Art Detection. However, the edge results in this case is missing some details of the person, and the TV monitor is almost absent. The red shapes indicate the missing details in the image. This loss of information also occurs when using HED or Canny edge. These weaknesses result in mislabeling in the synthetic image compared to the original image. We observe that the segmentation labels divide the regions of the labeled so their prior visualization accurately describes the label information in the original image. Therefore, the combination of the prior visual image I_i (\mathcal{V}_i^I) and prior visual segmentation label \mathcal{S}_i (\mathcal{V}_i^S) ensures that the generated image has a clear layout and well pre-

serves the labeled information. Our proposed combines \mathcal{V}_i^I and \mathcal{V}_i^S by a weighted sum:

$$\mathcal{V}_i^* = \omega_1 \mathcal{V}_i^I + \omega_2 \mathcal{V}_i^S \quad (4)$$

With ω_1, ω_2 being the trade-off scales when combining \mathcal{V}_i^I and \mathcal{V}_i^S . This combination results in a prior visual that is clear in content and complete information about labeled classes. Figure 3b shows an example of how the Visual Prior Combination method can be used to highlight classes in a dataset.

3.3 Create class balancing dataset

Algorithm 1: Class balancing algorithm for dataset generation

```

Input: Original dataset  $\mathcal{D}_{origin}$ ; Target
         images per class  $n_{balance}$ 
Output: Balanced dataset  $\mathcal{D}_{final}$ 
1 Stage 1: Initialization /* Storing
   images per class */
2  $\mathcal{M} \leftarrow \emptyset$ 
3 for  $I$  in  $\mathcal{D}$  do
4   for  $C$  in  $I$  do
5      $\mathcal{M}[C] \leftarrow \mathcal{M}[C] \cup \{I\}$ 
6 Stage 2: Sorting /* Sorting by number
   of classes */
7 for  $C$  in  $\mathcal{M}$  do
8   Sort  $\mathcal{M}[C]$ 
9 Stage 3: Balancing /* Generating
   additional images */
10  $\mathcal{D}_{gen} \leftarrow \emptyset$ 
11 for  $C$  in  $\mathcal{M}$  do
12   while  $\text{len}(\mathcal{M}[C]) < n_{balance}$  do
13     for  $I$  in  $\mathcal{M}[C]$  do
14       Generate  $I_{gen}$  based on  $I$ 
15        $\mathcal{M}[C] \leftarrow \mathcal{M}[C] \cup \{I_{gen}\}$ 
16        $\mathcal{D}_{gen} \leftarrow \mathcal{D}_{gen} \cup \{I_{gen}\}$ 
17       if  $\text{len}(\mathcal{M}[C]) \geq n_{balance}$  then
18         break
19  $\mathcal{D}_{final} \leftarrow \mathcal{D}_{gen} \cup \mathcal{D}_{origin}$ 
20 return  $\mathcal{D}_{final}$ 

```

To address the issue of class imbalance during model training, we aim for the final dataset \mathcal{D}_{final} , which merges the original dataset \mathcal{D}_{ori} and the synthetic dataset \mathcal{D}_{gen} , to have a balanced distribution among classes. To create a balanced dataset from the original dataset \mathcal{D}_{ori} , we use the class balancing algorithm to generate the dataset \mathcal{D}_{gen} based on the balancing factor $n_{balance}$, as presented in Algorithm 1. The

Table 1: Comparison in mIoU on val set between training of models on real training set and extended training set

Dataset		VOC7			VOC12		
Number images		209	92	183	366	732	1464
DeepLabV3+ Resnet50	D_{origin}	46.54	29.91	38.21	49.40	58.20	61.84
	$D_{gen} \cup D_{origin}$	49.72	33.87	41.45	52.22	60.11	63.06
	Δ	$\uparrow 3.18$	$\uparrow 3.96$	$\uparrow 3.24$	$\uparrow 2.78$	$\uparrow 1.91$	$\uparrow 1.22$
PSPNet Resnet50	D_{origin}	47.04	31.87	38.96	46.62	57.48	62.39
	$D_{gen} \cup D_{origin}$	50.01	34.67	41.46	49.34	61.09	63.78
	Δ	$\uparrow 2.97$	$\uparrow 2.80$	$\uparrow 2.50$	$\uparrow 2.72$	$\uparrow 3.61$	$\uparrow 1.39$
Mask2Former Resnet50	D_{origin}	48.28	34.85	39.63	51.37	59.94	63.65
	$D_{gen} \cup D_{origin}$	49.69	35.53	40.29	51.77	60.02	62.56
	Δ	$\uparrow 1.41$	$\uparrow 0.68$	$\uparrow 0.69$	$\uparrow 0.40$	$\uparrow 0.08$	$\downarrow 1.09$

algorithm consists of three main stages: Initialization, Sorting, and Balancing. In Stage 1, a dictionary \mathcal{M} is initialized to map each class to its associated images. Each image I is linked to a list of classes it contains. In the next stage, images are arranged in ascending order based on the number of classes they represent, prioritizing those with fewer classes to be generated to maintain the balance. In the final stage, additional images are generated for each class until they reach n_{gen} , ensuring an even distribution across classes. This process ensures the dataset is balanced, preventing overrepresentation of any class and promoting more robust model training.

After generating high-quality training samples, the synthetic dataset D_{gen} and the original dataset D_{origin} are merged into an extended dataset D_{final} for training:

$$D_{final} = D_{gen} \cup D_{origin} \quad (5)$$

In the default setting, we choose an appropriate n_{gen} such that $|D_{gen}|$ approx $|D_{origin}|$ where $|\cdot|$ is the number of images in the dataset. In Section 4.3.2, we further discuss changing the number of synthetic images generated.

4 RESULTS

4.1 Experiment Details

4.1.1 Dataset

In this section, we evaluate our method on the segmentation datasets VOC7 and VOC12 (Everingham et al., 2015). PASCAL VOC 2007 has 422 images annotated for semantic segmentation, split into

209 training and 213 validation images. Meanwhile, VOC12 has training and validation sets, including 1.464 and 1.449 images. In addition to training on the entire VOC12 dataset (1.464 images), we also train our model using 1/2 (732 images), 1/4 (366 images), 1/8 (183 images), and 1/16 (92 images) partition protocols (Wang et al., 2022). Evaluating our method on these few-sample datasets demonstrates its effectiveness in real-world scenarios.

4.1.2 Implementation details

We construct our framework on the deep learning PyTorch framework (Paszke et al., 2019) and T2I-Adapter (Mou et al., 2023) using Stable Diffusion XL 1.0 (Podell et al., 2024) with 30 time steps. We generate data using values for ω_1 and ω_2 , as defined in Section 4.3. For semantic segmentation, we employ the DeepLabV3+ (Chen et al., 2018), PSPNet (Zhao et al., 2017), and Mask2Former (Cheng et al., 2022) with segmenters implemented in the MMSegmentation framework (MMSegmentation Contributors, 2020). We utilize the SGD optimizer with standard settings in MMSegmentation. We train our models with an input image size of 512×512 on the Pascal VOC datasets, including VOC7 and VOC12. The performance of the trained model on the applied data is assessed using the Mean Intersection over Union (mIoU) metric.

4.2 Main Results

4.2.1 Quantitative results:

The results presented in Table 1 demonstrate that combining augmented data with the original dataset improves the performance of various segmentation models on the VOC7 and VOC12 datasets.



Figure 4: Some results show the limitations of direct generation and the ability of our method to overcome them.

All models, including DeepLabV3+, PSPNet, and Mask2Former, significantly improve when augmented data. DeepLabV3+ consistently performs the best across different dataset sizes. We note that as the amount of real-world data increases, the accuracy of the generated images and labels becomes crucial. Mismatched generated images in the synthetic data can lead to performance degradation; this is observed in Mask2Former when trained on the VOC12 dataset with 1464 images.

4.2.2 Qualitative results

In Figure 4, each row presents three images: the original image, the image generated by the original generative model, the description generated by BLIP2, and the image generated by the generative model combined with our method. The first two rows illustrate cases where the labeled classes in the image are either missing from the description or incorrectly described. This causes the model to either fail to generate those classes correctly (row 1) or produce images with blurred or unrecognizable objects (row 2). In the last row, the image is rather simple, and the prompt includes all labeled classes, but the generated image is still incorrect. With our pipeline, all three images have significantly improved with certain objects being fully generated and correctly positioned. This demonstrates that our method can effectively overcome the limitations of directly using the controllable imaging model.

Table 2: Impact of Class-Prompt Appending (1), Visual Prior Combination (2), Class balancing algorithm (3), and Post Filter (Fang et al., 2024) (4).

(1)	(2)	(3)	(4)	mIoU (%)
				42.15
✓				47.60
	✓			47.25
✓	✓			48.98
✓	✓	✓		49.72
✓	✓	✓	✓	51.23

Table 3: Effect of the number of synthetic data generated on data balance and performance.

n_{gen}	R/S	Entropy \uparrow	CLR \downarrow	mIoU (%)
-	209/0	3.944	0.253	46.54
27	209/216	4.044	0.231	49.72
41	209/425	4.042	0.231	50.37
55	209/634	4.059	0.224	49.25

4.3 Ablation Study

We conduct all ablation study experiments using the DeepLabV3+ model, backbone Resnet50 with training and evaluation details described in Section 4.1.2. The model is trained on the PASCAL VOC7 dataset, and the results are evaluated on the val set.

4.3.1 Effects of different methods:

The performance of the proposed methods is summarized in Table 4.3.1. When using the Baseline with generated prompts, the performance is only as low

Table 4: Performance of different text prompt selections

Method	Example	mIoU (%)
Generated caption	A room with a table and a laptop on it	47.24
Simple text prompt	A photo of sofa, chair, dining table	48.71
Class-Prompt Appending	A room with a table and a laptop on it; sofa, chair, dining table	49.72

as 42.15 % mIoU, which is lower than when training on the original data. This demonstrates the essential nature of the proposed methods when generating synthetic data. Our method yields a 49.72 % mIoU, showing its effectiveness. Additionally, we experimented with combining the Post Filter with the Category-Calibrated CLIP Rank (Fang et al., 2024) for generating synthetic data. The result of this combination is higher, which shows that our method can combine filters from previous studies (Fang et al., 2024; Wu et al., 2024) to improve the performance.

4.3.2 Effect of number of synthetic data:

The results of the proposed method’s experiments with different amounts of generated synthetic data are summarized in Table 3, **R/S** refers to the number of real/synthetic images. The metrics we use to evaluate data imbalance include Entropy, and Class Imbalance Ratio (CIR). First, when not training on synthetic data, the result is 46.54 mIoU. When training the model using synthetic data with a quantity of approx $|D_{origin}|$, approx $2 \times |D_{origin}|$, and approx $3 \times |D_{origin}|$, the data balance metrics remain stable at a better level than before; the model performance is also better. We found that the amount of synthetic data approx $3 \times |D_{origin}|$ has affected the model performance when the performance is now lower than when the number is approx $1 \times |D_{origin}|$, approx $2 \times |D_{origin}|$.

4.3.3 Text prompt selection:

Table 4 compares different text prompt selection methods for generative modeling. We compare the performance of three prompt types: *Generated caption generated* from the image captioning model, *Simple text prompt* listing the classes in the image, and *Class-Prompt Appending*, a combination of the two prompt types. *Class-Prompt Appending* outperforms the other two methods by 49.72, precisely 3.20 and 1.80 better than Generated caption and Simple text prompt, respectively, in mIoU. These results show that the *Class-Prompt Appending* text prompt selection method can support SD in generating diverse datasets and ensuring accurate attention.

Table 5: Study on different trade-off scales

ω_2	ω_1				
	0.6	0.7	0.8	0.9	1.0
0.7	47.12	47.32	46.42	45.36	45.38
0.8	48.51	48.93	48.32	47.09	46.79
0.9	49.13	49.72	49.11	48.79	48.36
1.0	48.13	49.32	48.91	48.33	47.03

4.3.4 Effect of different trade-off scales:

Trade-off scales are utilized to combine the visual prior of the image with the semantic segmentation map presented in Section 3.2.2. We tested various scales and documented the results in Table 5. The outcomes indicate that the scale $\omega_1=0.7$ and $\omega_2=0.9$ yields the best results, with ω_2 enabling proper localization of the labeled classes. On the other hand, the scale $\omega_1=0.7$ retains the general content of the image without needing to be as detailed as the original image.

4.3.5 Other Visual Priors

We compare using different visual priors for both T2I-Adapter (Mou et al., 2023) and ControlNet (Zhang et al., 2023): Line Art (Chan et al., 2022), Canny (Canny, 1986), Sketch (Su et al., 2021). We also combine Inpainting (Rombach et al., 2022) with our methods (excluding Visual Prior Combination). Although the T2I-Adapter combined with Line Art gives the best result at 49.72% mIoU, other visual priors also show competitive performance, especially Canny on both T2I-Adapter and ControlNet. Figure 5 shows some imaging results with controllable diffusion model.



Caption: *Caption a room with a table and a laptop on it*

Class labels: *sofa, chair, dining table*

Figure 5: Some image generation results from various methods when combined with our proposed approach.

Table 6: Different visual priors controlled the enhancement results. All used the Stable Diffusion XL model.

	T2I-Adapter			ControlNet	Inpainting
	LineArt	Canny	Sketch	Canny	
mIoU (%)	49.72	48.95	47.52	48.95	47.56

5 DISCUSSION AND CONCLUSION

5.1 Limitations

While our approach effectively generates synthetic images to augment data for semantic segmentation, there are certain limitations to consider. First, the results in Tables 1, 3 show that the model’s performance may decrease when the number of synthetic images is large or more significant than the number of original real images. This may be because the synthetic images do not completely guarantee the original images’ location and quantity of labels. Additionally, as the images produced by the Stable Diffusion (Podell et al., 2024) model are trained on the LION-5B dataset (Schuhmann et al., 2022), the resulting images do not share the same distribution as the target dataset. So, the synthetic data cannot completely replace the original training dataset used to train the model.

5.2 Conclusion

We introduce a data augmentation pipeline based on a controllable diffusion model for semantic segmentation tasks. Our evaluations were performed on the PASCAL VOC dataset, and the results show that our pipeline significantly improves the performance of semantic segmentation models. We note that our method can be combined with other data augmentation methods to enhance performance further. This

significant advancement opens the door for future research into data augmentation using generative models.

REFERENCES

- Azizi, S., Kornblith, S., Saharia, C., Norouzi, M., and Fleet, D. J. (2023). Synthetic data from diffusion models improves imagenet classification. *Transactions on Machine Learning Research*.
- Canny, J. (1986). A computational approach to edge detection. *IEEE Transactions on Pattern Analysis and Machine Intelligence*, PAMI-8(6):679–698.
- Chae, J., Cho, H., Go, S., Choi, K., and Uh, Y. (2023). Semantic image synthesis with unconditional generator. In *Thirty-seventh Conference on Neural Information Processing Systems*.
- Chan, C., Durand, F., and Isola, P. (2022). Learning to generate line drawings that convey geometry and semantics. In *2022 IEEE/CVF Conference on Computer Vision and Pattern Recognition (CVPR)*, pages 7905–7915.
- Chen, L.-C., Zhu, Y., Papandreou, G., Schroff, F., and Adam, H. (2018). Encoder-decoder with atrous separable convolution for semantic image segmentation. In Ferrari, V., Hebert, M., Sminchisescu, C., and Weiss, Y., editors, *Computer Vision – ECCV 2018*, pages 833–851, Cham.
- Cheng, B., Misra, I., Schwing, A. G., Kirillov, A., and Girdhar, R. (2022). Masked-attention mask transformer for universal image segmentation. In *2022 IEEE/CVF Conference on Computer Vision and Pattern Recognition (CVPR)*.
- Everingham, M., Eslami, S. M. A., Gool, L. V., Williams,

- C. K. I., Winn, J., and Zisserman, A. (2015). The pascal visual object classes challenge: A retrospective. *International Journal of Computer Vision*, 111(1):98–136.
- Fang, H., Han, B., Zhang, S., Zhou, S., Hu, C., and Ye, W.-M. (2024). Data augmentation for object detection via controllable diffusion models. In *2024 IEEE/CVF Winter Conference on Applications of Computer Vision (WACV)*, pages 1246–1255.
- He, R., Sun, S., Yu, X., Xue, C., Zhang, W., Torr, P., Bai, S., and Qi, X. (2023). IS SYNTHETIC DATA FROM GENERATIVE MODELS READY FOR IMAGE RECOGNITION? In *The Eleventh International Conference on Learning Representations*.
- Ho, J., Jain, A., and Abbeel, P. (2020). Denoising diffusion probabilistic models. In *Advances in Neural Information Processing Systems*, volume 33, pages 6840–6851.
- Li, J., Li, D., Savarese, S., and Hoi, S. (2023). Blip-2: bootstrapping language-image pre-training with frozen image encoders and large language models. In *Proceedings of the 40th International Conference on Machine Learning, ICML’23*.
- Lin, T.-Y., Maire, M., Belongie, S., Hays, J., Perona, P., Ramanan, D., Dollár, P., and Zitnick, C. L. (2014). Microsoft coco: Common objects in context. In *Computer Vision – ECCV 2014*, pages 740–755, Cham. Springer International Publishing.
- MMSegmentation Contributors (2020). OpenMMLab Semantic Segmentation Toolbox and Benchmark.
- Mou, C., Wang, X., Xie, L., Wu, Y., Zhang, J., Qi, Z., Shan, Y., and Qie, X. (2023). T2i-adapter: Learning adapters to dig out more controllable ability for text-to-image diffusion models.
- Nguyen, Q. H., Vu, T. T., Tran, A. T., and Nguyen, K. (2023). Dataset diffusion: Diffusion-based synthetic data generation for pixel-level semantic segmentation. In *Thirty-seventh Conference on Neural Information Processing Systems*.
- Paszke, A., Gross, S., Massa, F., Lerer, A., Bradbury, J., Chanan, G., Killeen, T., Lin, Z., Gimelshein, N., Antiga, L., Desmaison, A., Kopf, A., Yang, E., DeVito, Z., Raison, M., Tejani, A., Chilamkurthy, S., Steiner, B., Fang, L., Bai, J., and Chintala, S. (2019). Pytorch: An imperative style, high-performance deep learning library. In *Advances in Neural Information Processing Systems*, volume 32.
- Podell, D., English, Z., Lacey, K., Blattmann, A., Dockhorn, T., Müller, J., Penna, J., and Rombach, R. (2024). Sdxl: Improving latent diffusion models for high-resolution image synthesis. In *The Twelfth International Conference on Learning Representations*.
- Ranftl, R., Lasinger, K., Hafner, D., Schindler, K., and Koltun, V. (2022). Towards robust monocular depth estimation: Mixing datasets for zero-shot cross-dataset transfer. *IEEE Transactions on Pattern Analysis and Machine Intelligence*, 44(3).
- Rombach, R., Blattmann, A., Lorenz, D., Esser, P., and Ommer, B. (2022). High-resolution image synthesis with latent diffusion models. In *Proceedings of the IEEE/CVF Conference on Computer Vision and Pattern Recognition (CVPR)*, pages 10684–10695.
- Schuhmann, C., Beaumont, R., Vencu, R., Gordon, C. W., Wightman, R., Cherti, M., Coombes, T., Katta, A., Mullis, C., Wortsman, M., Schramowski, P., Kundurthy, S. R., Crowson, K., Schmidt, L., Kaczmarczyk, R., and Jitsev, J. (2022). LAION-5b: An open large-scale dataset for training next generation image-text models. In *Thirty-sixth Conference on Neural Information Processing Systems Datasets and Benchmarks Track*.
- Su, Z., Liu, W., Yu, Z., Hu, D., Liao, Q., Tian, Q., Pietikäinen, M., and Liu, L. (2021). Pixel difference networks for efficient edge detection. In *2021 IEEE/CVF International Conference on Computer Vision (ICCV)*, pages 5097–5107.
- Trabucco, B., Doherty, K., Gurinas, M. A., and Salakhutdinov, R. (2024). Effective data augmentation with diffusion models. In *The Twelfth International Conference on Learning Representations*.
- Wang, Y., Wang, H., Shen, Y., Fei, J., Li, W., Jin, G., Wu, L., Zhao, R., and Le, X. (2022). Semi-supervised semantic segmentation using unreliable pseudo labels. In *Proceedings of the IEEE/CVF International Conference on Computer Vision and Pattern Recognition (CVPR)*.
- Wu, W., Dai, T., Huang, X., Ma, F., and Xiao, J. (2024). Gpt-prompt controlled diffusion for weakly-supervised semantic segmentation.
- Xie, S. and Tu, Z. (2015). Holistically-nested edge detection. In *2015 IEEE International Conference on Computer Vision (ICCV)*, pages 1395–1403.
- Yu, F., Chen, H., Wang, X., Xian, W., Chen, Y., Liu, F., Madhavan, V., and Darrell, T. (2020). Bdd100k: A diverse driving dataset for heterogeneous multitask learning. In *IEEE/CVF Conference on Computer Vision and Pattern Recognition (CVPR)*.
- Zhang, L., Rao, A., and Agrawala, M. (2023). Adding conditional control to text-to-image diffusion models. In *2023 IEEE/CVF International Conference on Computer Vision (ICCV)*, pages 3813–3824.
- Zhao, H., Shi, J., Qi, X., Wang, X., and Jia, J. (2017). Pyramid scene parsing network. In *Proceedings of the IEEE Conference on Computer Vision and Pattern Recognition (CVPR)*.
- Zhou, B., Zhao, H., Puig, X., Xiao, T., Fidler, S., Barriuso, A., and Torralba, A. (2019). Semantic understanding of scenes through the ade20k dataset. *International Journal of Computer Vision*, 127(3):302–321.